Nuclear Inst. and Methods in Physics Research, A 997 (2021) 165162

Contents lists available at ScienceDirect

Nuclear Inst. and Methods in Physics Research, A

journal homepage: www.elsevier.com/locate/nima

# Study of silicon photomultiplier performance at different temperatures

N. Anfimov *, D. Fedoseev, A. Rybnikov, A. Selyunin, S. Sokolov, A. Sotnikov

*Joint Institute for Nuclear Research, Joliot-Curie 6, Dubna, 141980, Russia*

ARTICLE INFO

*Keywords:*
Silicon photomultiplier — SiPM
Photon detection efficiency — PDE
Dark Count Rate — DCR
PDE temperature dependence

ABSTRACT

Decrease in operating temperature of a silicon photomultiplier (SiPM) reduces its dark noise. Some experiments consider low temperatures to take advantage of this possibility. And one of them is the TAO detector. It requires operation at $T \approx -50$ °C. In this paper, the studies of operation of both Hamamatsu SiPMs and AdvanSID SiPMs in a temperature range of −100 °C to +23 °C are presented.

## 1. Introduction

A silicon photomultiplier (SiPM) is an array of small avalanche photodiodes called pixels which operate above the breakdown voltage in the Geiger mode. The breakdown voltage is the minimum reverse bias voltage which leads to self-sustaining avalanche multiplication in every SiPM pixel. The voltage above the breakdown is called overvoltage (OV). Such a structure allows detecting and working with very low-intensity light in a proportional mode in a range limited by the total number of pixels. Nowadays, SiPMs are widely used in different areas, for instance, in experimental physics and medical diagnostic equipment. High detection efficiency, insensitivity to magnetic fields, a compact size and a gain of up to $10^6$ are the main advantages of SiPMs over conventional photomultipliers. However, there are some drawbacks of SiPMs, such as the high dark count rate, the optical crosstalk and temperature dependence of some parameters.

At present, a new satellite experiment, the TAO experiment, is under consideration [1] to accompany the JUNO neutrino project [2]. The TAO detector, intended to precisely measure the spectrum of primary neutrinos from nuclear reactors, is a spherical vessel filled with liquid scintillator and covered by photosensors. To achieve the required energy resolution of less than 2% at 1 MeV for the TAO experiment, light detection efficiency should be maximized, and the noise level minimized. A SiPM with its high photon detection efficiency (PDE) is a good candidate for the TAO detector. To reduce the high noise level of SiPMs, it is proposed to operate the TAO detector at low temperature $T \approx -50$ °C [3]. However, one relevant study [4] observed a significant PDE drop of the $1 \times 1$ mm$^2$ FBK-IRST SiPM type T6-V1-PD at $T \approx -50$ °C ($\approx 220$ K) (see Fig. 1). Such a drop can totally wash out the advantage of using SiPMs. Also, some studies [5–7] demonstrate that temperature can affect PDE. The same impact might be found in other SiPM models. In this study, two SiPM models have been examined, Hamamatsu MPPC-S13360-6025CS [8] (a single SiPM) and AdvanSID ASD-NUV4S-P-4x4TD [9] (only one SiPM on the array).

The paper is organized as follows. Section 2 introduces the experimental setup. Section 3 represents data analysis methods and the results.

## 2. Experimental setup

A Dewar's vessel is used as a cryostat to keep liquid nitrogen (LN). Nitrogen vapor produces in the Dewar a temperature gradient at different heights (from room temperature to that of liquid nitrogen). A SiPM can be set at any of these heights. In this study, the height is chosen to provide the minimum temperature. We can change the sample temperature merely by heating it up, without any displacement, to guarantee reliability and consistency of our measurements. To prevent ambient light penetration, the Dewar vessel is placed in a dark, completely light-tight room.

### 2.1. Incident light stability

To make the study reliable, light intensity should be kept stable in time and not affected by ambient changes. A stabilized LED light source with a wavelength of 425 nm produced by the HVSys company [10] was used in this study. The LED of this kind provides stable light intensity. The LED light is transported to SiPM via the plastic optical fiber TORAY PFU-CD1001-22-E. We have observed that light traveling through the optical fiber can vary in intensity by about 10% depending on temperature changes from room temperature to −100 °C. The reason could be changes in optical properties of the fiber core and the cladding. To get rid of these nuisance effects, the temperature along the fiber length is stabilized, which allows keeping the fiber at room temperature.

* Corresponding author.
*E-mail address:* anphimov@jinr.ru (N. Anfimov).

https://doi.org/10.1016/j.nima.2021.165162
Received 26 May 2020; Received in revised form 2 January 2021; Accepted 17 February 2021
Available online 19 February 2021
0168-9002/© 2021 Elsevier B.V. All rights reserved.

**Table 1**
Breakdown voltages for the AdvanSid ASD-NUV4S-P-4 × 4TD SiPM at different temperature points extracted by ILD test and quadratic fit.

| Extraction method | Breakdown voltage $V_{bd}$ at different temperatures | | |
|---|---|---|---|
| ILD test | 26.57 ± 0.03 V[ 23 °C]<br>24.58 ± 0.03 V[−52 °C] | 26.02 ± 0.03 V[ 2 °C]<br>23.83 ± 0.03 V[−84 °C] | 25.39 ± 0.03 V[−22 °C] |
| Quadratic fit | 26.55 ± 0.02 V[ 23 °C]<br>24.57 ± 0.02 V[−52 °C] | 26.00 ± 0.02 V[ 2 °C]<br>23.84 ± 0.02 V[−84 °C] | 25.39 ± 0.02 V[−22 °C] |

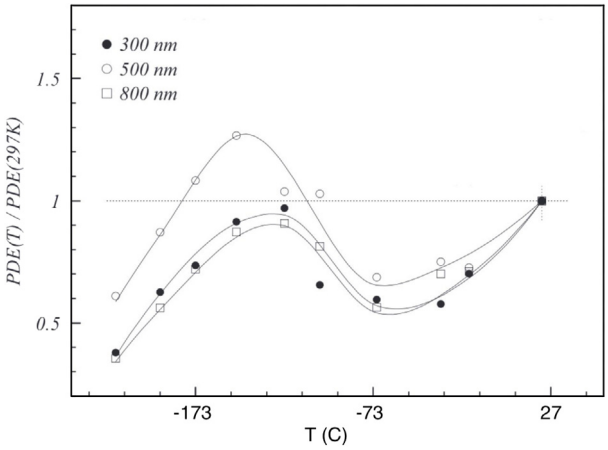



**Fig. 1.** Normalized photon detection efficiency as a function of temperature for fixed overvoltage of 2 V and three wavelengths (300 nm, 500 nm, and 800 nm) for a 1 × 1 mm$^2$ FBK-IRST SiPM type T6-V1-PD [4].

### 2.2. Setup description

The cryostat vessel of ∼ 30 liters is filled to about 1/3 with liquid nitrogen (see Fig. 2a). The assembly of a light delivery system (see Fig. 2b) with a SiPM (called further a probe) is moving along the cryostat depth. The light delivery system is a bundle of six optical fibers placed inside a copper pipe. The light is sent to the SiPM or a reflective plate (in case of calibration) through the central fiber. Then, the light reflects and travels to other 5 fibers used to monitor the light stability by the temperature change. The pipe is wound with a heating cable, the feedback is provided via a thermal sensor in the pipe. The heating cable keeps the fiber bundle at a stable temperature. Additionally, the assembly is thermally insulated from outside.

The reflective plate is placed in front of the fiber bundle to calibrate light stability. Quite high light intensity is used enough to monitor the reflected light by means of the PIN-photodiode ThorLabs FDS100-CAL [11] and the Keithley 6487 Picoammeter/Voltage source. The measurement gives an estimation of light stability at different ambient temperatures. The overall light stability in our system reached the level of 1%.

Then, the reflection plate is replaced with a single SiPM glued to the aluminum substrate (bed) with thermal grease and an embedded thermosensor on its backside. For the AdvanSID SiPM array, a copper cylinder is used. The SiPM array and the thermosensor are placed inside the copper cylinder which is wound with a heating cable (see Fig. 3). Temperature stability is guaranteed with a precision better than 1 °C in both cases.

The testing procedure is the following:

- The SiPM probe[1] is put at a minimum temperature height (∼ −100°C).
- The probe is heated up by adjusting the current in heating cables. Temperatures are monitored by two thermosensors.
- The system is calibrated by using the small reflective plate and high light intensity (enough to read out the current from the monitoring photodiode). During the measurements at different temperatures, current fluctuations obtained with the Keythley 6487 picoammeter are less than 1%.
- The reflective plate is replaced by a SiPM (or array). We also checked the consistency with the calibration by measuring the reflected light from the SiPM. And then, the LED was switched into a single photon mode.

[1] Copper pipe with fibers + SiPM on the bed or on the copper cylinder.

### 2.3. Readout chain and data acquisition

The readout chain of measurements consists of a SiPM power supply source, an amplifier, and a high-speed digitizer (see Fig. 4). Apart from the readout chain, two power sources supply the heating cables. All of these pieces of equipment are located outside the darkroom, except the amplifier and the Dewar.

To provide the bias voltage to the SiPM, the Keithley 6487 is used. The source automatically measures SiPM current–voltage ($I$–$V$) curves determining the breakdown voltage.

The SiPM signal is digitized by means of the DRS4 [12] evaluation board which can sample a signal within a range of (0.7–5) GS/s with an about 11.5 effective bit precision. It operates in the external trigger mode and is synchronized with the LED trigger signal. The accumulated data is analyzed using the ROOT package software [13]. In order to distinguish single photoelectrons, a high-gain amplifier (two cascades of OPA847 by Texas Instruments) is put into the readout chain to increase the ADC sensitivity by 225 times.

## 3. Data analysis and results

### 3.1. PDE evaluation

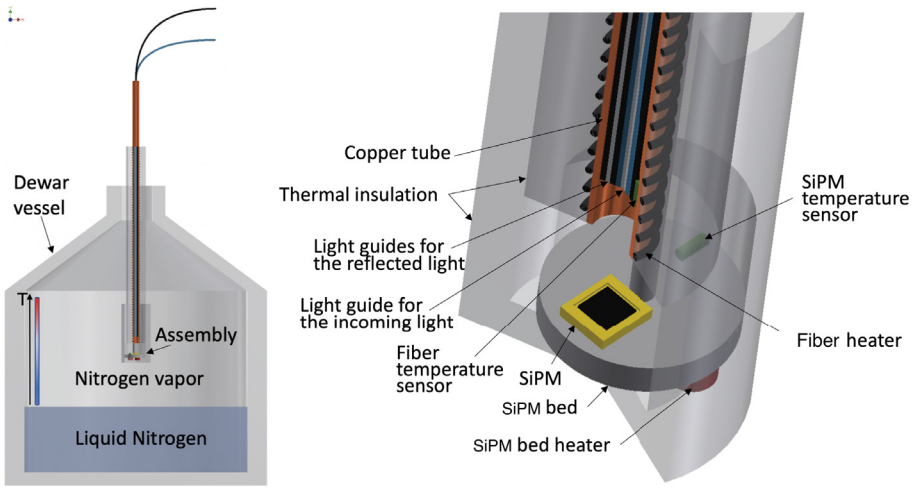
By integrating waveforms within a fixed window (gate), SiPM charge spectra can be extracted.[2] We acquire $N$-events for the signal spectrum (LED is ON), see Fig. 5a, and $D$-events for the dark spectrum (LED is OFF). Using the number of events in the pedestal $N_0$ for the signal spectrum (shaded area under the pedestal peak) and $D_0$ for the dark spectrum (shaded area given in the same range), the average number of photoelectrons $\hat{\mu}$ can be estimated [14]

$$\hat{\mu} = -\ln\left(\frac{N_0}{N}\cdot\frac{D}{D_0}\right) = -\ln\left(\frac{\hat{p}_{\xi_0}}{\hat{p}_{\lambda_0}}\right) = \hat{\xi} - \hat{\lambda}, \tag{1}$$

where $\hat{p}_{\xi_0}$, $\hat{p}_{\lambda_0}$ - estimators of the pedestal probability in the signal and dark spectra, and $\hat{\xi} = -\ln(\hat{p}_{\xi_0})$, $\hat{\lambda} = -\ln(\hat{p}_{\lambda_0})$ - estimators of the average number of photoelectrons in the signal and dark spectra, respectively. Statistical errors in this case can be evaluated [14]

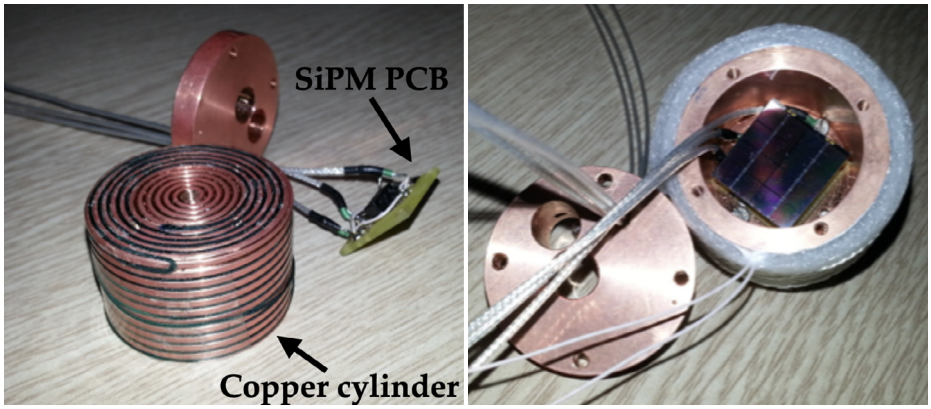
$$\frac{\hat{\sigma}_{\hat{\mu}}}{\hat{\mu}} \approx \frac{1}{\sqrt{N}}\sqrt{\frac{e^{\hat{\xi}} + e^{\hat{\lambda}} - 2}{(\hat{\xi} - \hat{\lambda})^2}}. \tag{2}$$

[2] A SiPM charge spectrum usually provides better single electron resolution compared to its amplitude spectrum (see Fig. 5b). The charge spectra allow better extraction of pedestal events. We put the pedestal cut at 3$\sigma$ back from the first peak position $Q_1$ (see Fig. 5a), which provides systematic uncertainty in the pedestal event extraction less than 1%.




(a) (b)

**Fig. 2.** Schematic view of the experimental setup: a – Dipped probe into the Dewar vessel, b – Probe schematic with SiPM bed and light guides are mounted in a copper tube.




(a) (b)

**Fig. 3.** Copper cylinder is wound with heating cable and PCB with ASD-NUV4S-P-4x4TD: a — side view, b — top view.

### 3.2. Breakdown voltages

To compare parameters at different temperatures, a SiPM should be operated with similar overvoltage. One of the ways to find the breakdown voltage is to analyze the $I$–$V$ curve of a SiPM. There are several approaches to breakdown voltage extraction. In the study, the inverse logarithmic derivative (ILD) test [15] was used. The ILD for $I$–$V$ curve reads

$$f(V) = \left[\frac{1}{I} \cdot \frac{dI}{dV}\right]^{-1} \tag{3}$$

and the minimum of the $f(V)$ yields the inflection point, which defines the breakdown voltage. For the AndvanSid SiPM, the quadratic fit from the paper [4] was also used. Both approaches demonstrate good consistency of breakdown voltage extraction (see Table 1). The voltages measured for both SiPMs using the ILD test are shown in Fig. 6. These results are in a good agreement with [16].

### 3.3. DCR evaluation

The Dark Count Rate (DCR) of SiPMs is evaluated in the following way. By processing raw waveforms, we count the number of dark pulses (LED is OFF) that exceed some fixed threshold. We process $w = 10000$ waveforms within the duration window $W = 1.024$ μs[3] (1024 samples, 1 GS/s sampling rate). We use a pulse shape confirmation procedure, which allows counting signals only with the shape structure identical to SiPM signals. Also, this procedure takes into account the overlapping of the signals and the fact that some signals are partially present in the waveform window (in this case we shrank the window by the pulse

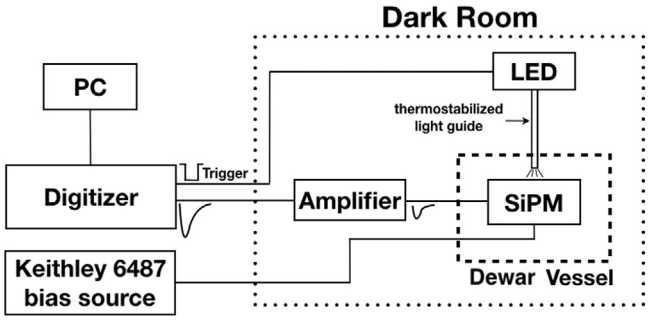
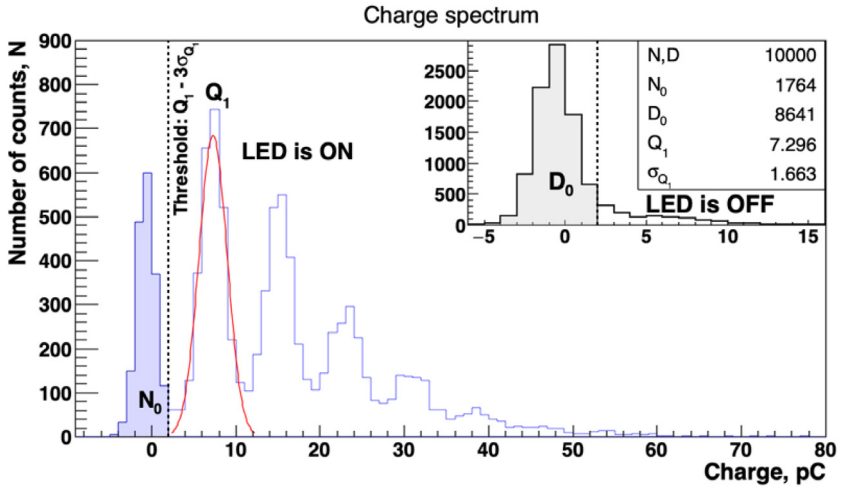
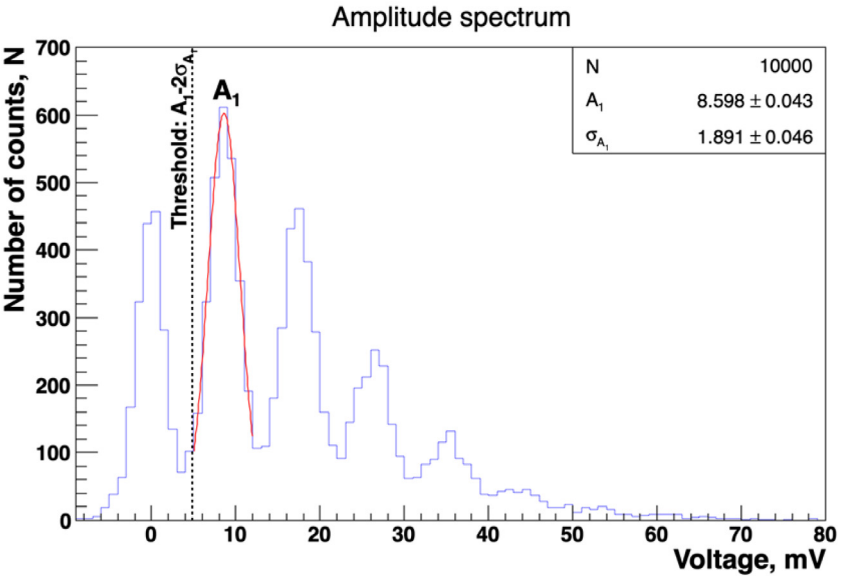



**Fig. 4.** Readout chain circuit.

[3] In our case, SiPM pulses ~ 100 ns (FWHM) which can introduce a small fraction of pulses miscounting.




(a)




(b)

**Fig. 5.** Typical charge and amplitude spectra of SiPMs: a — charge spectrum illustrates the pedestal method for evaluation of an average number of photoelectrons. Shaded area and $N_0$ — pedestal events on signal spectrum, shaded area and $D_0$ — pedestal events on dark spectrum (incorporated picture); b — amplitude spectrum of SiPM and an illustration of the threshold extraction method for DCR evaluation.

width). The overall counting window is $w \times W$. The DCR rate $R$ can be found from the number of dark pulses $N$ that are counted in the overall window as

$$R = \frac{N}{w \times W} \tag{4}$$

The number of random pulses $N$ follow the Poisson distribution[4] and standard deviation of the DCR using Eq. (4) is

$$\sigma_R = \frac{\sqrt{N}}{w \times W}. \tag{5}$$

The threshold is obtained as an empirical compromise between efficiency and noise pickup. By measuring the SiPM amplitude spectra (see. Fig. 5b), we define the optimal threshold[5] $T$ as

$$T = A_1 - 2\sigma_{A_1}, \tag{6}$$

where $A_1$ and $\sigma_{A_1}$ - the amplitude and its standard deviation of the single photoelectron signal, respectively. Threshold decrease leads to significant noise pickup at a small gain (overvoltage). In our case (see Eq. (6)), only ~2.5% of the SiPM signals are miscounted in the dark rate evaluation procedure.[6]

### 3.4. Results

The PDE and DCR measurements have been performed for both SiPM samples at different temperatures and in the range of operating overvoltages. To present PDE more illustratively, it is normalized to 25% (see Fig. 7) for the Hamamatsu SiPM ($V_{OV}$ = 5.0 V at $T$ = 23.0 °C) and to 42%[7] for the ASD-NUV4S-P-4x4TD ($V_{OV}$ = 5.68 V at $T$ = 23.0 °C).

[4] Standard deviation $\sigma_N = \sqrt{N}$.

[5] Assuming signal and noise pulses are of similar amplitude.

[6] Assuming single pixel's amplitudes follow Normal distribution.

[7] On Fig. 7b, PDE is a bit higher than 40% at $V_{OV}$ = 6 V. For our sample, we were not able to reach $V_{OV}$ above 5.68 V because of the high noise level. And assumed PDE = 42% at this point.

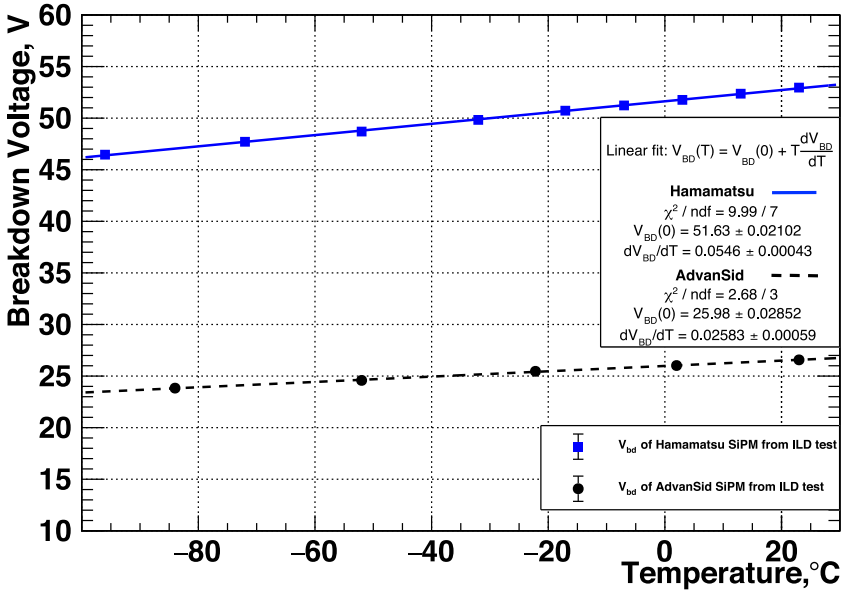
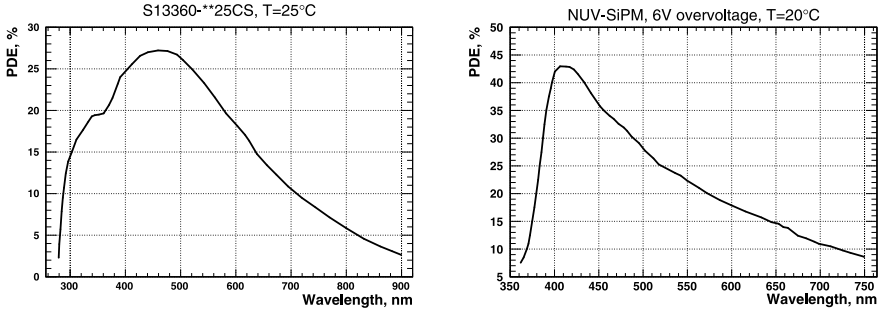



**Fig. 6.** Breakdown voltages[8] for Hamamatsu and AdvanSid SiPMs vs temperature using ILD test (see Eq. (3)).




(a) (b)

**Fig. 7.** PDE as a function of wavelength: a – for the Hamamatsu SiPM at overvoltage OV = 5 V [8], b – for the AdvanSid SiPM at OV = 6 V [9].

In general, the setup and techniques demonstrated in this paper allow measuring different SiPM types in a wide range of temperatures, from that of liquid nitrogen (77 K) up to room temperature.

The PDE and DCR dependencies on overvoltage for both SiPMs have been studied in a range of temperatures from $T = +23.0$ °C (room temperature) down to $T \approx -100.0$ °C.

To compare the results of the PDE behavior at all temperatures, it is plotted as a function of overvoltage (see Fig. 8). The presented results with uncertainty less than 10% allow excluding temperature dependence on PDE for both samples.

The DCR for SiPMs (see Fig. 9) decreases rapidly and reaches the drop by a factor of several orders of magnitude at low temperatures compared to room conditions. This fact is one of the major considerations for SiPMs to employ them in the TAO detector at $T = -50$ °C. The DCR values[9] cannot be extracted for low overvoltages at negative temperatures (see Fig. 9).

The presented results show that SiPMs are good candidates to be used as photodetectors in the TAO experiment.

[8] Error bars are less than the size of the points.

[9] Small number of dark pulses comparing to a noise pickup at a very low threshold.

## CRediT authorship contribution statement

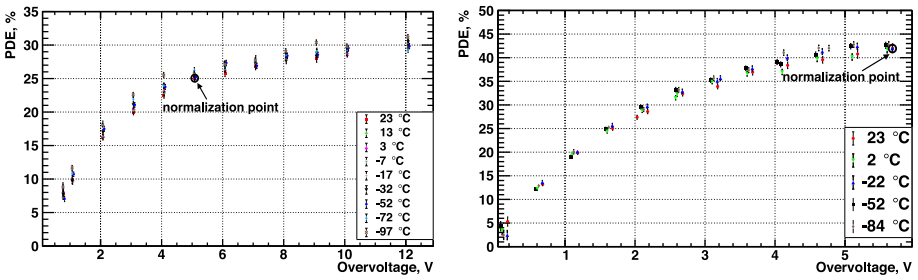
**N. Anfimov:** Supervision, Conceptualization, Methodology, Writing - original draft, Writing - review & editing, Project administration. **D. Fedoseev:** Methodology, Resources. **A. Rybnikov:** Software, Formal analysis, Investigation, Visualization. **A. Selyunin:** Methodology, Writing - original draft, Writing - review & editing, Investigation, Formal analysis, Visualization. **S. Sokolov:** Methodology, Visualization, Resources. **A. Sotnikov:** Software, Formal analysis, Investigation, Methodology.

## Declaration of competing interest

The authors declare that they have no known competing financial interests or personal relationships that could have appeared to influence the work reported in this paper.

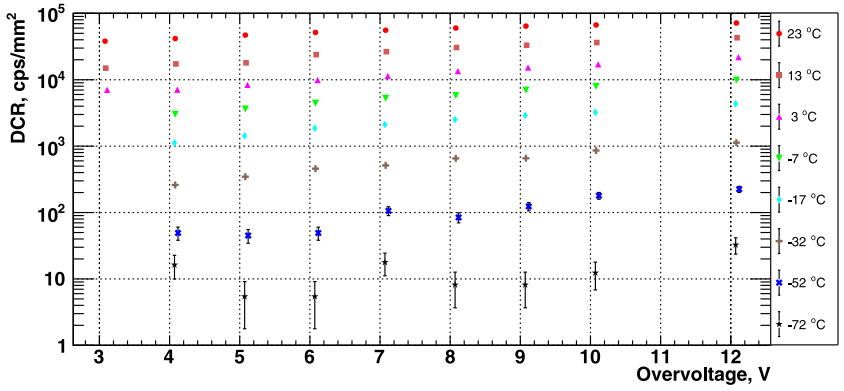
## Acknowledgments

The authors are indebted to Dr. Dmitry Naumov, Prof. Alexander Olshevskiy and Natalia Mazarskaya from the Joint Institute for Nuclear Research for their great help in the preparation of this paper. This work is supported by the Russian Science Foundation under grant 21-42-00023

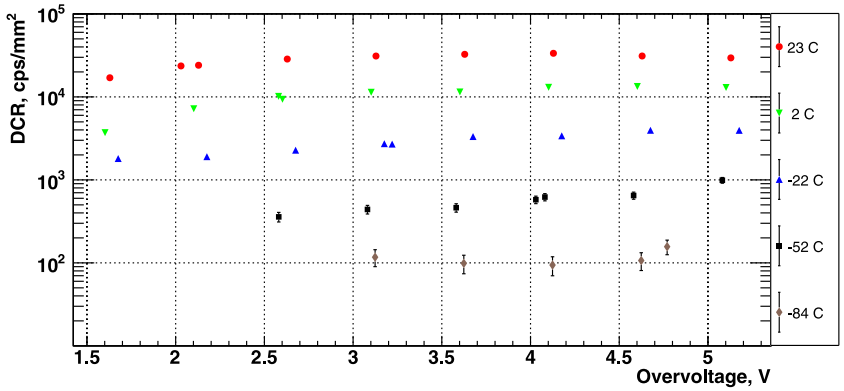



(a) (b)

**Fig. 8.** PDE ($\lambda = 425$ nm) as a function of overvoltage at different temperatures: a — for Hamamatsu SiPM, b — for AdvanSid SiPM.




(a)




(b)

**Fig. 9.** DCR as a function of overvoltage: a — for Hamamatsu SiPM, b — for AdvanSid SiPM.

## References


[1] A. Abusleme, et al., JUNO Collaboration, TAO Conceptual design report, 2020, arXiv:2005.08745.

[2] Z. Djurcic, et al., JUNO Collaboration, JUNO Conceptual design report, 2015, arXiv:1508.07166.

[3] G. Cao, JUNO-TAO experiment with large area high performance SiPMs, in: SiPM Workshop, Vienna, 2019.

[4] G. Collazuol, M. Bisogni, S. Marcatili, C. Piemonte, A. Del Guerra, Studies of silicon photomultipliers at cryogenic temperatures, Nucl. Instrum. Meth. A628 (1) (2011) 389–392, http://dx.doi.org/10.1016/j.nima.2010.07.008, VCI 2010.

[5] R. Iwai, M. Sakurai, A. Antognini, I. Belosevic, M. Hildebrandt, K. Kirch, A. Knecht, A. Papa, A. Stoykov, Characterization of cryogenic SiPM down to 6.5K, JPS Conf. Proc. 27 (2019) 012005, http://dx.doi.org/10.7566/JPSCP.27.012005.

[6] M. Biroth, P. Achenbach, E. Downie, A. Thomas, Silicon photomultiplier properties at cryogenic temperatures, in: R. Barbier, et al. (Eds.), Nucl. Instrum. Methods A 787 (2015) 68–71, http://dx.doi.org/10.1016/j.nima.2014.11.020.

[7] P. Lightfoot, G. Barker, K. Mavrokoridis, Y.A. Ramachers, N. Spooner, Characterisation of a silicon photomultiplier device for applications in liquid argon based neutrino physics and dark matter searches, J. Instrum. 3 (2008) P10001, http://dx.doi.org/10.1088/1748-0221/3/10/P10001.

[8] Hamamatsu, MPPC S13360-6025cs, 2019, https://www.hamamatsu.com/eu/en/product/type/S13360-6025CS/index.html.

[9] AdvanSiD, ASD-NUV4S-P-4x4TD, 2019, http://advansid.com/products/product-detail/asd-sipm4s-p-4x4td.

[10] HVSys, Calibrated LED sources of light flashes, 2019, http://hvsys.ru/images/data/news/5_small_1368802948.pdf.

[11] ThorLabs, FDS100-CAL - calibrated si photodiode, 2019, https://www.thorlabs.com/thorproduct.cfm?partnumber=FDS100-CAL.

[12] P.S. Institute, DRS4 evaluation board, 2019, https://www.psi.ch/en/drs/evaluation-board.

[13] R. Brun, F. Rademakers, ROOT - An object oriented data analysis framework, Nucl. Instr. and Meth. A 389 (1997) 81–86, http://dx.doi.org/10.1016/S0168-9002(97)00048-X.

[14] N. Anfimov, A. Rybnikov, A. Sotnikov, Optimization of the light intensity for photodetector calibration, Nucl. Instrum. Meth. A939 (2019) 61–65, http://dx.doi.org/10.1016/j.nima.2019.05.070, http://www.sciencedirect.com/science/article/pii/S0168900219307260.

[15] V. Chmill, E. Garutti, R. Klanner, M. Nitschke, J. Schwandt, Study of the breakdown voltage of SiPMs, in: Proceedings, 14th Vienna Conference on Instrumentation (VCI 2016): Vienna, Austria, February 15-19, 2016, Nucl. Instrum. Meth. A845 (2017) 56–59, http://dx.doi.org/10.1016/j.nima.2016.04.047.

[16] T. Cervi, M. Bonesini, A. Falcone, A. Menegolli, G.L. Raselli, M. Rossella, M. Torti, Performances of some sipm models for cryogenic applications, Nucl. Instrum. Methods Phys. Res. A 912 (2018) 326–328, http://dx.doi.org/10.1016/j.nima.2017.12.011, New Developments In Photodetection 2017.